AMAS Workshop on Modelling in Biomechanics
MiB'03 – (pp.159–189) – Warsaw, April 7–11, 2003.

Modelling of the response of cells to mechanical stimulation

P. J. PRENDERGAST, D. J. KELLY and J. G. McGARRY

Centre for Bioengineering
Department of Mechanical Engineering
Trinity College, Dublin, Ireland
pprender@tcd.ie

Physical stimuli act at all levels in the biological system, from the whole organ level down to individual molecules. The effect of these stimuli for the health of tissues is currently the subject of intense investigation, and it is one of the growing application areas for applied mechanics. In this paper, a synopsis of these investigations is given, followed by a description of mechano-regulation of bone remodelling and tissue differentiation. An attempt is made to present a generalized approach for simulation of mechano-regulation in the form of evolution equations: these equations are then tested against observations that have been made during specific processes known to be mechanoregulated (fracture healing and osteochondral defect healing). From the results of these simulations, some speculations on future problems in computational mechanobiology and their potential solutions are made.

The full solution of problems in modelling cell behaviour might be best achieved by explicitly modelling cell behaviour. Explicit treatment of cells can be made by modelling the cell features as a continuum, or alternatively by considering the cytoskeletal elements as tensegrity structures. An approach combining tensegrity and continuum modelling using finite element analysis is presented. The confirmation of such an approach by comparison with atomic force microscopy is attempted. Finally, an analyses of the application of fluid flow and substrate strain on single cells is given. Some possibilities of explicit modelling of cells in culture in the context of mechanoregulation are discussed.

1. Introduction

Mechanical forces constantly act on tissues and organs. Sometimes the consequences of mechanical forces are obvious, such as when a bone fractures or a ligament is injured by over-stretching. Such problems have long been the subject of investigation – even Galileo thought about what forces would break bones of different sizes (Ascenzi, 1993). However, mechanical forces also have more subtle consequences. They may act within tissues at the

cellular level to regulate biological processes; this aspect of biomechanics has recently been given the name *mechanobiology*. In *Skeletal Function and Form* Carter & Beaupré (2001) give many examples of mechanobiology of skeletal development, aging, and regeneration. Van der Meulen & Huiskes (2002) have presented a review of the literature of both experimental and computational studies in mechanobiology. Experimental studies use living tissues: e.g. in the case of skeletal mechanobiology, a fractured long bone can be exposed to various levels of bending and the corresponding tissue formation observed. In computational mechanobiology the problem may be split into two parts:

(i) solution of the boundary value problem to determine local mechanical stimuli within the domain,

(ii) development of equations to relate the local mechanical stimuli to cell expression which creates tissue with a functional matrix composition and structure.

The first part of the computational mechanobiology problem involves determination of suitable constitutive models that not only account for macroscopic stress/strain behaviour but also allow determination of the mechanical or biophysical stimuli acting within the tissue at a cellular level. For bone or cartilage, poroelasticity theories have been proposed to analyze fluidic stimulation and straining of the cells within the tissues, e.g. Cowin (1999) and Mow et al. (1980). The second part of the computational mechanobiology problem involves the derivation of the equations that describe the relationship between the rates of change of tissue properties as a function of the mechanical stimuli. These mechano-regulation rules have been proposed for growth, adaptation, regeneration (repair), and degeneration of tissues (Carter & Beaupré, 2001; Prendergast & Contro, 2002).

Section 2 of this paper presents a brief introduction of the kind of problems we wish to solve in mechanobiology. Section 3 presents the theoretical development of evolution equations for tissue adaptation and regeneration. Because explicit modelling of cells may lead to a better understanding of how mechanical forces elicit a biological response from a cell, Sec. 4 describes how an individual cell may be modeled. Section 5 discusses how these modelling approaches may be combined in future studies.

2. Some relevant literature

Growth, adaptation, remodelling and degeneration of tissues involve processes that either change tissue from one type to another or resorb it altogether. We can consider a domain filled with biological tissue as a reactive continuum. Parts of the domain will change from one tissue type to

another. One cell type that is central to this process is the *stem cell*, the parent cell from which the cells that generate connective tissues differentiates. The concept of a stem cell originated in the early 20^{th} Century (Bianco & Robey, 2001). Recently researchers have attempted to elucidate what controls stem cell differentiation. It has been suggested that chemical and mechanical stimuli can control the differentiation of skeletal stem cells (also called mesenchymal stem cells) into either fibrous connective tissue, cartilaginous tissue, bone, or adipose tissue (Caplan, 1994), see Fig. 1.

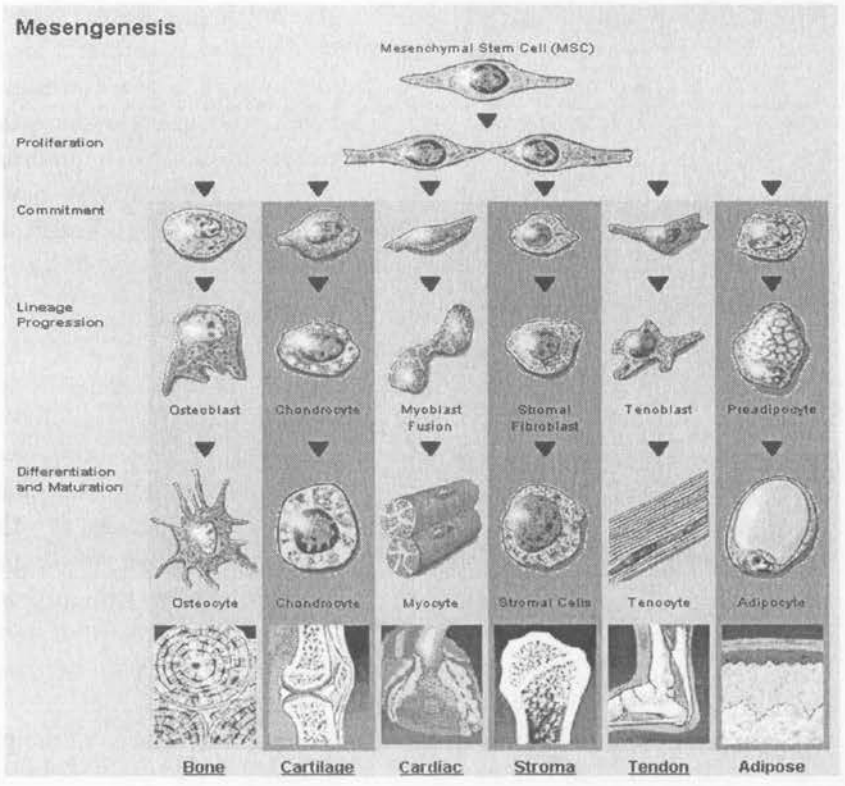

FIGURE 1. Differentiation pathways for mesenchymal stem cells.

The first papers describing the adaptation of a *continuum* to a change in load were by Cowin and co-workers, beginning with Cowin & Hegedus (1976). In that work, an adaptive elasticity theory was proposed whereby a unit of bone tissue was modeled as an open system, and an evolution equation for the rate of change of density as a function of the strain was developed. Adaptive elasticity, and the numerical implementations of it, did not rely explicitly on knowledge of how cells responded to strain, but rather approached the prob-

lem according to classical continuum mechanics. The continuum approach was often used over the next two decades until the papers of Weinans et al. (1994) showed that an instability in local remodelling could generate a pattern analogous to a trabecular bone network. Although the instability was attributed to the discretization of the finite element mesh and was therefore inadmissible, Jacobs et al. (1995) showed that a similar process occurred even if these numerical problems were corrected. Later Huiskes et al. (2002) showed how explicit modelling of cell behaviour could be used to predict trabecular bone remodelling in response to changes in the applied load.

Tissue differentiation is the replacement of one tissue phenotype by another and it is partly regulated by mechanical epigenetic factors. This has been known for a long time; for example from the work of the German orthopaedic surgeon Friedrich Pauwels (1885-1980) who showed that tissue types within a healing fracture callus could be correlated with the hydrostatic or deviatoric nature of the stress on the mesenchymal cell pool. Several computational schemes have been proposed to simulate tissue differentiation – for a description of these the reader is referred to Prendergast & Van der Meulen (2001).

3. Evolution equations for tissue differentiation

When considering a mathematical framework for simulating mechano-regulated biological processes, it can be noted that the processes are thermodynamically irreversible (Weinans & Prendergast, 1996). In this respect, it is appropriate to consider equations of evolution which describe in precise terms the way these processes evolve. And to quote Fung (1965), "...some new hypotheses must be introduced, whose justification can only be sought by comparing any theoretical deductions with experiments".

Stem cells differentiate into the cells that produce the various tissue phenotypes of interest (*i.e.*, the connective tissues, which are fibrous connective tissue, fibrocartilage, cartilage, and bone). Therefore we must compute a distribution of cells throughout the continuum. If n^i denotes the number of cells of the i^{th} type then,

$$\frac{\mathrm{d}n^i}{\mathrm{d}t} = D^i \nabla^2 n^i + P^{\mathrm{i}}(S).n^{\mathrm{i}} - K^i(S).n^i, \tag{3.1}$$

where D^i is a diffusion coefficient for cell i, $P^i(S)$ is a proliferation rate and $K^i(S)$ is an apoptosis (death) rate for cell i as a function of the stimulus S.

If ϕ_j denotes the volume fraction of tissue j then

$$\sum_{j=1}^{n_t} \phi_j = 1, \tag{3.2}$$

where n_t is the number of tissue types. The diffusion coefficient of cells of type i through a volume of tissue can be approximated as the weighted average of the tissue types present in the volume, i.e.

$$D^i = \sum_{j=1}^{n_t} D_{ij}\phi_j, \tag{3.3}$$

D_{ij} being the diffusion rate of cell i in tissue j. The proliferation rate may be independent of the stimulus or, more generally, an optimal stimulation for proliferation may exist requiring a relationship of the form:

$$P^i(S) = a_i + b_i S + c_i S^2. \tag{3.4}$$

Whether or not a stem cell will differentiate into a fibroblast to form fibrous connective tissue, a chondrocyte to form cartilage, or an osteoblast to form bone, is hypothesized to depend on the stimulus, S. This is a central tenant of mechanobiology, promoted by the concepts of Caplan (1994) and assumed by researchers in the field; see Prendergast & Van der Meulen (2001). It can be written as:

$$\begin{aligned} 0 \leq S < n &\quad \text{bone resorption,} \\ n \leq S < 1 &\quad \text{bone,} \\ 1 \leq S < m &\quad \text{cartilage,} \\ m \leq S &\quad \text{fibrous connective tissue,} \end{aligned} \tag{3.5}$$

where the stimulus S is a function of the biophysical stimuli on the cells that will change the stem cell shape or otherwise stimulate the cell (Huiskes et al., 1997). It is not possible to determine what these stimuli may be *a priori*; instead some new hypothesis must be introduced and its validity assessed by comparing predictions with observations.

The specific hypothesis we introduce is that substrate strain and fluid flow are the primary biophysical stimuli for stem cell differentiation. This hypothesis is proposed based on empirical evidence that differentiated cells respond to biophysical stimuli, e.g., Kaspar et al. (2000) placed osteoblasts on a plate subjected to four–point bending and recorded increases in matrix synthesis (collagen Type I) and reductions in the synthesis of certain signaling molecules; in a similar experiment, Owan et al. (1997) found that fluid flow

was a dominant stimulus over substrate strain. Klein-Nulend et al. (1996) analyzed a layer of osteocytes, osteoblasts, and fibroblasts and found that osteocytes generated increased signaling molecules (PGE_2) in response to pulsatile fluid flow and decreased in response to hydrostatic pressure;

A poroelastic theory is used to compute the fluid flow and substrate strain in the tissue, and these are used as a basis for the stimulus as follows:

$$S = \frac{\gamma}{a} + \frac{v}{b}, \tag{3.6}$$

where γ is the shear strain and v is the fluid velocity, a and b being empirical constants. To derive an evolution equation, the magnitude of the stimulus needs to be related to the rate of tissue formation. If it is assumed that the rate of change of tissue density ρ is a function of the difference between the actual stimulus and the homeostatic stimulus ΔS then:

$$\frac{\mathrm{d}\rho_i}{\mathrm{d}t} = f(\Delta S, n_i). \tag{3.7}$$

Detailed forms of Eq. (3.7) have been proposed for bone, that is for $0 \leq S < n$, (the bone resorption field) and $n \leq S < 1$ (the bone formation field). In particular, the rate of bone formation and the rate of bone resorption have been described by Carter (1984) as non-linear functions of strain with a "zone" of homeostatic equilibrium, or a "lazy zone", i.e.

$$\frac{\mathrm{d}\rho}{\mathrm{d}t} = \begin{cases} f_1(S) & S < S_{\min}, \\ 0 & S_{\min} < S < S_{\max}, \\ f_2(S) & S > S_{\max}. \end{cases} \tag{3.8}$$

In Prendergast (2002), the specific formulation of Eq. (3.8) was developed to include microdamage as a stimulus. Using the concept [Prendergast & Taylor (1994)] that damage accumulation is a stimulus for bone remodelling, it can be noted that, if the repair rate in bone is not fast enough to repair damage as it forms, then damage will accumulate. This net damage will reduce the Young's modulus of the matrix surrounding a cell and cause a reduction in the stress sensed by the cells leading to resorption. Therefore, because of the influence of damage, bone resorption occurs at high strain levels. This will result in an evolution equation of the form plotted as in Fig. 2.

If this concept can be extended to all connective tissues, then a superimposed set of evolution equations could be developed to predict the evolution of all tissue phenotypes under the influence of the stimulus as shown in Fig. 3.

The set of evolution equations represented in Fig. 3 will ensure resorption of all connective tissue when $S < S_{\mathrm{a}}$, maintenance of bone and resorption

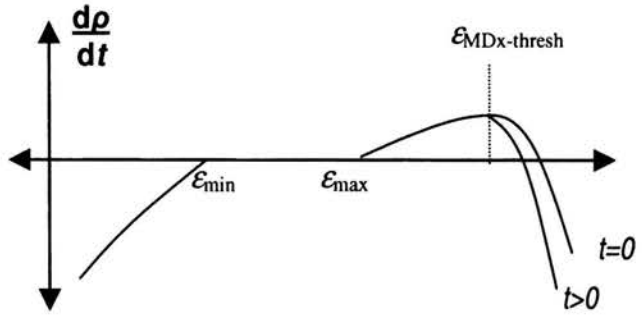

FIGURE 2. The evolution of bone density as a function of the stimulus (the stimulus is strain only in this case), from Prendergast (2002). Because damage accumulates with strains greater than $\varepsilon_{MDx\text{-}thresh}$ the curve in that region is time dependent.

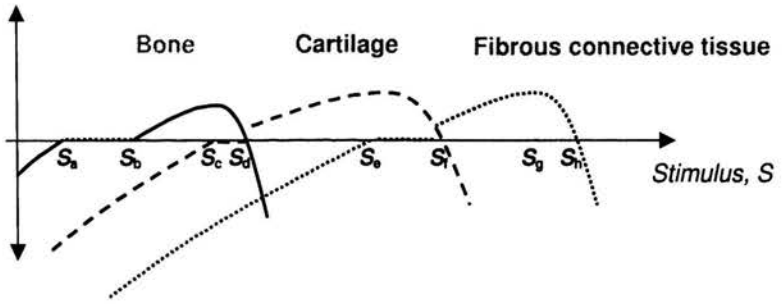

FIGURE 3. A representation for hypothesized evolution functions for connective tissue.

of cartilage and fibrous connective tissue if $S_a < S < S_b$, formation of bone at an ever increasing rate, and resorption of cartilage and fibrous connective tissue if $S_b < S < S_c$, damage accumulation in bone and a reduced bone formation rate, maintenance of cartilage, and resorption of fibrous connective tissue if $S_c < S < S_d$, resorption of bone and fibrous connective tissue and formation of cartilage at an ever increasing rate for $S_d < S < S_e$, and so on. It must be stated that the set of evolution equations represented by Fig. 3 is highly speculative and serves mainly to represent the nature of the problems awaiting solution in computational mechanobiology.

3.1. Computational implementation

In the case of regeneration of bone, we may let i take the values as follows:

1 = stem cells (precursor cells),

2 = fibroblasts,

3 = chondrocytes,

4 = osteoblasts.

The first author's research group have considered two analyses of bone regeneration; long bone fracture repair (Lacroix et al., 2002, Lacroix & Prendergast, 2002a, 2002b) and osteochondral defect healing (Kelly & Prendergast, 2003).

3.1.1. Fracture repair. When a long bone such as the tibia is fractured an inflammation phase immediately begins and granulation tissue containing mesenchymal stem cells originating in either from the medullary cavity, the external muscle, or the surface of the bone (cadmium layer of the periostium), enters the fracture callus. Various tissues are generated in an orchestrated sequence leading to eventual healing of the bone. To simulate this process according to the formulation described in Sec. 3 above, Eq. (3.1) was simplified to

$$\frac{\mathrm{d}n}{\mathrm{d}t} = D\nabla^2 n, \tag{3.9}$$

such that proliferation and apoptosis were neglected. It was assumed that the only cell that differentiated was the stem cell. In these simulations, the constants were

$$\begin{aligned} a &= 3.75\%, \\ b &= 3.0\,\mu\mathrm{m\ s}^{-1}, \\ n &= 0.01, \\ m &= 3.0 \end{aligned} \tag{3.10}$$

and the diffusion constant was taken as $D = 0.34\ \mathrm{mm}^2$ per day. An axisymmetric finite element model of a fracture callus was generated, and a poroelastic model of the tissues were used to calculate apparent level fluid flow and tissue strains.

Equation (3.6), with the constants as given in Eq. (3.10), was used to determine which tissue will form at a site (element) in the model. The evolution equations had the character of an algorithm where by if S exists at a site (i.e. in an element) for more than some transformation time, then tissue j is generated such that $\phi_{i=j} = 1$ and $\phi_{i\neq j} = 0$. Clearly this kind of evolution equation assumes immediate transformation of the tissue at a site, which is only good as a first approximation. This computational scheme was set

up in an iterative procedure. Beginning with a fracture callus formed from granulation tissue post-inflammation phase, the sequence of tissue formations and resorption leading to a head bone was simulated in both 2D (Lacroix & Prendergast, 2002a), and in 3D (Lacroix & Prendergast, 2002b).

3.1.2. Osteochondral defect repair. It sometimes occurs that the cartilage layer on a bone surface becomes damaged and in need of repair. The repair procedure can involve a surgical technique whereby the subchondral bone below the defect is drilled, a cell-seeded scaffold is placed in the defect, and it is expected that the new load-bearing tissue will eventually form in the defect. Kelly and Prendergast (2003) report an attempt to simulate this process by considering cell proliferation into the defect filled with granulation tissue, followed by dispersion of cells according to Eq. (3.1) whereby proliferation, differentiation, and apoptosis is a function of the stimulus. The proliferation equation of Eq. (3.4) is written as:

$$\frac{\mathrm{d}}{\mathrm{d}t}\begin{Bmatrix} n^1 \\ n^2 \\ n^3 \\ n^4 \end{Bmatrix} = \begin{bmatrix} a_1 & b_1 & c_1 \\ a_2 & b_2 & c_2 \\ a_3 & b_3 & c_3 \\ a_4 & b_4 & c_4 \end{bmatrix} \begin{Bmatrix} 1 \\ S \\ S^2 \end{Bmatrix}, \tag{3.11}$$

where

$$\begin{bmatrix} a_1 & b_1 & c_1 \\ a_2 & b_2 & c_2 \\ a_3 & b_3 & c_3 \\ a_4 & b_4 & c_4 \end{bmatrix} = \begin{bmatrix} a_{\text{stem cell}} & 0 & 0 \\ a_{\text{fibroblast}} & b_{\text{fibroblast}} & c_{\text{fibroblast}} \\ a_{\text{chondrocyte}} & 0 & 0 \\ a_{\text{osteoblast}} & 0 & 0 \end{bmatrix}. \tag{3.12}$$

To simulate the process, an axi-symmetric poroelastic finite element model of an osteochondral defect within an idealised model of a femoral condyle was created. Initially the defect is cell free and filled with a granulation tissue. The mesenchymal cells are assumed to originate from the bone marrow (Fig. 4). The maximum octahedral shear strain and fluid flow within each element was calculated and depending on both stimuli the cellular dispersal, proliferation, differentiation and apoptosis was determined.

The pattern of repair predicted within the 5 mm defect did not vary greatly between the low density mesh and the high density mesh (Fig. 5a and Fig. 5b). Initially the defect is partially shielded from the load, and the primary stimulus within the defect is towards osteogenesis.

As the repair tissue begins to stiffen, it starts to support load, and significant chondrogenesis is predicted within the center of the defect, with fibrous tissue predicted to form at the articular surface and bone tissue predicted to

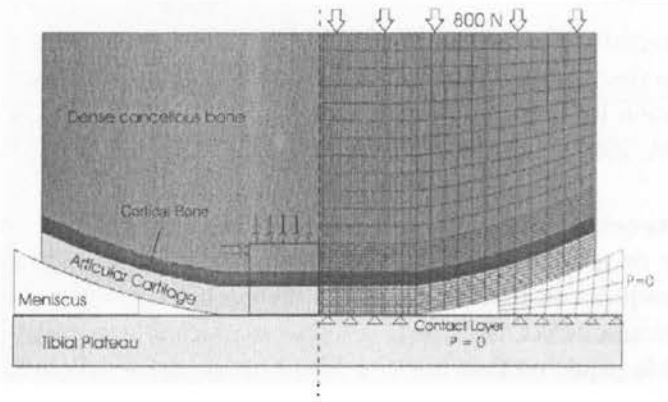

FIGURE 4. Axi-symmetric finite element model of the knee with an osteochondral defect. Right: Finite element mesh illustrating loading and boundary condition. Left: 5mm defect (box) showing source of mesenchymal cells (arrows).

form in the base of the defect through direct intramembranous ossification. As healing progresses increased bone formation is predicted to occur due to endrochonrdal ossification, and regions of cartilage begin to dedifferentiate into fibrous tissue, leading to an overall reduction in the amount of cartilage tissue observed within the defect. Fibrous or cartilaginous tissue is predicted to persist at the interface between the repair tissue and the residual tissue due to high fluid flows in this region.

4. Modelling of single cells

The challenge of developing a model for the biomechanical behaviour of a single cell has not yet been met. The model we have developed fuses two techniques of mechanics – continuum modelling and tensegrity modelling – to create a finite element model of a cell adherent to a substrate. Here we report on an attempt to confirm the finite element model by comparing its predictions of force/displacement responses with those obtained experimentally by indentation of a cell using the tip of an atomic force microscope. Atomic force microscopy (AFM; Binnig et al., 1986) has become a valuable tool for studying biological materials (Weisenhorn et al., 1993). It can be used to investigate the mechanical properties of adherent cells (Radmacher et al., 1996; Charras and Horton, 2002). For example, indenting the cell surface with the AFM tip to measure the force required for a certain depth of indentation. Despite technical difficulties of such measurements (Costa and Yin, 1999; Al-Hassan et al, 1998) replicating the indentation of the AFM probe in a structural model could, in principle, be used to confirm a biome-

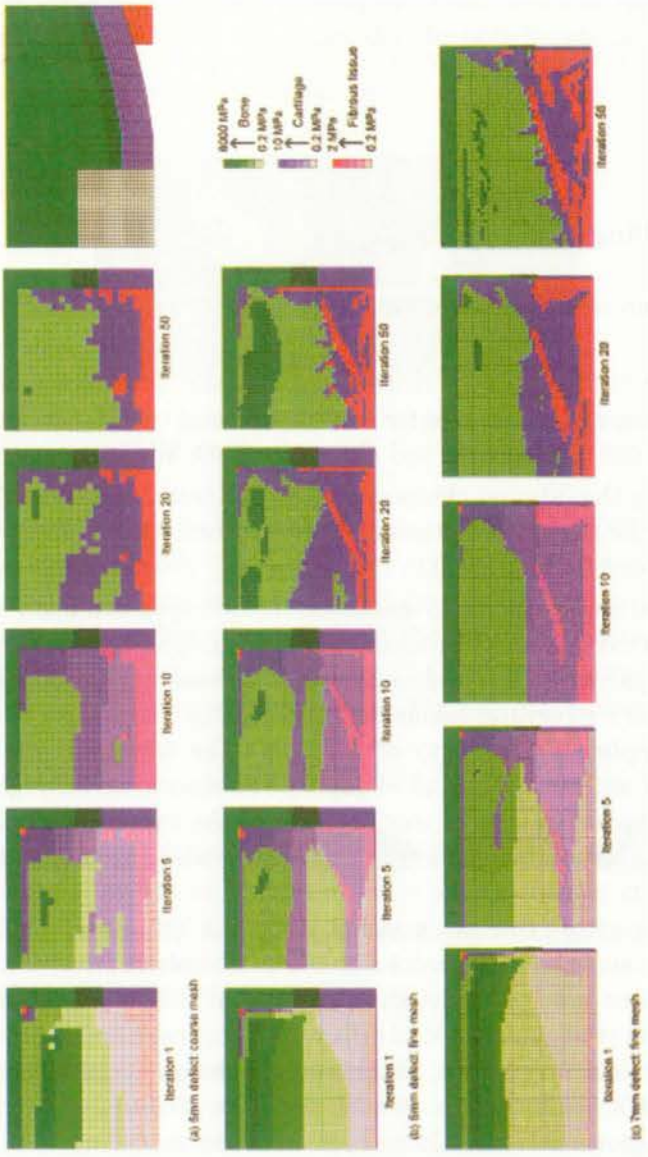

FIGURE 5. The osteochondral defect is given in the gray region in the inset of the figure on the top right hand corner. Noting the coloured bar which represents the different tissue types, we can see that (a) by comparing the first and second rows, the density of the finite element mesh does not have an appreciable influence on the outcome of the simulations and (b) comparing the second and third rows, a 5 mm and a 7 mm defect are predicted to behave similarly. The main result is that full bone healing is not predicted and that fibrous tissue persists on the surface where the cartilage should be.

chanical model of a cell. Next, we present preliminary results of simulating the mechanical stimulation of cells subjected to substrate strain and fluid flow.

4.1. Modelling approach

Biomechanical models of adherent cells have generally taken two different approaches:

(i) attributing the primary structural role to the cytoskeleton, and thereby assuming a minimal role for other aspects of cellular composition (Ingber, 1993; Stamenovic and Coughlin, 2000; Wendling et al., 1999).

(ii) treating the internal cytoplasm as a continuum and thereby assuming no role for the cytoskeleton in resisting deformation (Kamm et al., 2000; Evans and Yeung, 1989).

Structural models of the cytoskeleton include open-cell foam models and stress-supported tensegrity (tensional-integrity) approaches. The tensegrity approach in particular has had considerable success in describing certain features of a cell's structural behaviour, such as the increase in stiffness with increasing applied forces (Sato et al., 1990), the non-linear effects of prestress on cell stiffness (Wang et al., 2001; Stamenovic and Coughlin, 1999), experimental observations of reorientation of the cytoskeleton and nucleus when integrin receptors on the cell surface are pulled (Maniotis et al., 1994). Such observations support the view that rigid cytoskeletal networks can distribute forces within the cell, possibly through a balance of compression in microtubules and tension in microfilaments. The alternative continuum approach has been used to model airway epithelial cells in a 2D finite element model (Kamm et al., 2000), blood cells with a cortical membrane and viscous cytoplasm (Evans and Yeung, 1989), and the deformation of a chondrocyte within its extracellular matrix (Guilak and Mow, 2000).

Although some advances have been made in modelling the mechanical behaviour of adherent cells, we believe that models incorporating the main structurally-significant components of adherent cells would prove useful in exploring the biomechanical response of cells. Indeed, it has been suggested by Hochmuth (2000) that:

"the modelling of cellular deformation in the future may combine elements of both continuum models and tensegrity models. This may be especially important for cells attached to surfaces at points of focal adhesion where molecular cross bridging occurs".

4.2. Model geometry

A finite element model is developed to represent a spreading fibroblast adherent on a flat substrate, based on images of a spreading cell (Fig. 6).

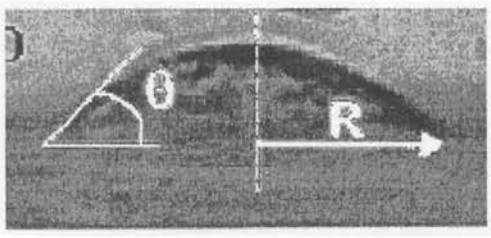

FIGURE 6. Image of a spreading chick embryo fibroblast on a glass microplate for 3 hours; adapted from [20].

Based on experimental observations (Thoumine et al., 1999), the volume of the cell is approximately 3,000 μm^3. The nucleus is formed from an ellipse with a major axis of 8 μm, minor axis of 5 μm, and a distance of 2 μm from the cell-substrate interface (Fig. 7a). Next the model comprises an internal cytoskeleton of tensile actin elements (Fig. 7b), and compressive microtubule elements (Fig. 7c), together with cytoplasm (Fig. 7d), and membrane (Fig. 7e) components.

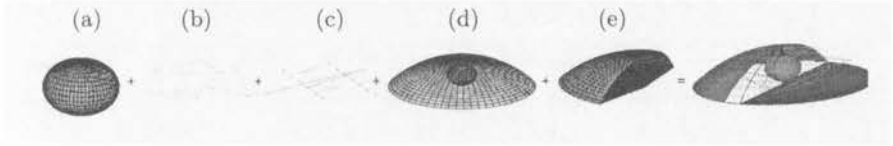

FIGURE 7. Illustration of the development of a 3D finite element model of a cell, incorporating the (a) nucleus, (b) network of microfilaments, (c) microtubules, (d) cytoplasm, (e) membrane.

The cytoskeleton consists of a network of six compression-bearing struts (two in each orthogonal direction) and 24 tensional cables. These represent the aggregate behaviour of microtubules and microfilaments respectively. The end of each strut connects with four cables at 12 common nodes, which are also coincident with membrane and underlying cytoplasm nodes, and are therefore analogous to 'receptor' sites or adhesion complexes in adherent cells. The microtubule and microfilament elements are altered in length and position from what was an originally rounded tensegrity structure (Fig. 8) to fit the more spread cell shape (Fig. 7).

New surface locations for the 'cytoskeleton' nodes are established by firstly determining the nodal positions that maintain the original vertical

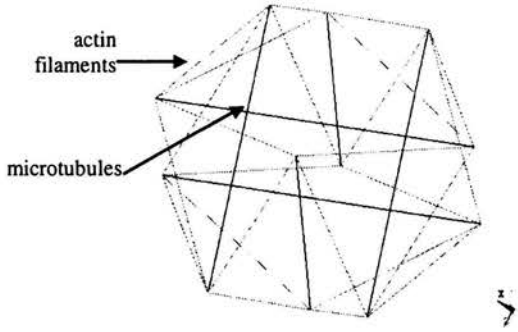

FIGURE 8. 3-dimensional tensegrity network of microtubules and microfilaments, representing the internal cytoskeleton.

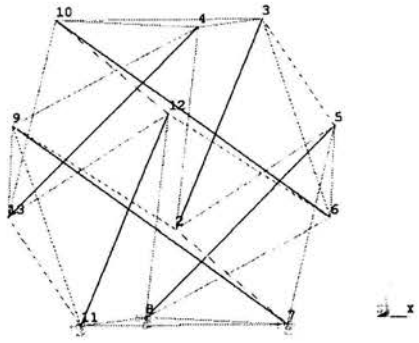

FIGURE 9. A plane representing the cell-substrate interface is established by applying constraints to end nodes (7, 8 and 11 in this diagram) of three microtubule struts, one strut from each orthogonal direction. The nine unconstrained nodes lie on unconstrained horizontal planes; nodes 2, 6, 13 nearest the substrate, nodes 5, 9, 12 next, and nodes 3, 4, 10 farthest from the substrate. These nodes are repositioned downwards to comply with the imposed spread shape to give the final configuration for a spread cell.

proportions of the internal structure in a rounded model, i.e. three horizontal planes (Fig. 9).

Radial planes defined by the central axis and the original nodal positions are then established; the intersection of these planes with the surface of the new spread model yields lines along which the new nodal positions must lie. Points of intersection of these surface lines with the three horizontal planes established yield nine new nodal positions of the cytoskeleton when repositioned to conform to the spread shape.

The cytoplasm and nucleus elements are meshed with 8-node lower-order hexahedral elements. The membrane is meshed with 4-node shell elements. Microtubule struts (Fig. 7c) and microfilament cables (Fig. 7b) are meshed with single link elements (a three-dimensional spar element with bilinear stiffness matrix), compression-only and tension-only respectively.

4.3. Constitutive modelling of cell elements

Material properties for each of the cell components are not known precisely and can only be estimated from various sources (Table 1). While generally accepted as being viscoelastic, the cytoplasm and nucleus are treated here as linear elastic and isotropic continua. Although this is a simplification of the complex material behaviour of both components, it is considered sufficient for describing static mechanical response and avoids incorporation of unknown non-linear material behaviour. The elastic modulus is chosen as 100 Pa in accordance with values used in Kamm et al. (2000). The nucleus has been reported as four times stiffer than the cytoplasm and is therefore given a value of 400 Pa. The Poisson's ratio (ν) for both nucleus and cytoplasm is chosen initially as 0.37 (Shin and Athanasiou, 1999). In the model developed in Kamm et al. (2000), epithelial cell membrane elasticity was specified as 10^7 Pa, with a thickness of 6 nm. Since in that study it was concluded that the membrane elastic properties were over-estimated, a lower value of 10^3 Pa (with $\nu = 0.3$) is chosen in the present model, while maintaining the same membrane thickness. The properties applied to the cytoskeleton components (Table 1) are based on elasticity values extracted from the flexural rigidity of microtubules and microfilaments subjected to thermal fluctuations (Gittes et al., 1993). On assumption of isotropy and homogeneity, microtubules and microfilaments are assigned cross-sectional areas (190 nm^2 and 18 nm^2 respectively) that correspond to the elasticity values in Table 1.

TABLE 1. Elastic properties assigned to the components in the model. (* $1 \cdot 10^{-10}$ $N/\mu m^2$; ¶ taken from Guilak et al., (2000); † taken from Kamm et al. (2000); § taken from Gittes et al. (1993).)

Component	Elastic modulus (Pa)	Poisson's ratio (ν)
Cytoplasm	100*	0.37
Nucleus¶	400	0.37
Membrane†	103	0.3
Microtubules§	$1.2 \cdot 109$	0.3
Microfilaments§	$2.6 \cdot 109$	0.3

4.4. Boundary conditions

All nodes (shell and solid), at the cell-substrate interface, including the three nodes that establish the cell-substrate plane in each model (Fig. 9), are constrained in all three translational degrees of freedom, and are therefore analogous to focal adhesion sites in adherent cells. Initial constraints in each analysis involve application of a prestress (an initial strain to account for the contractile effect of acto-myosin sliding mechanisms) to the microfilament elements. This initial strain exerts tension on the other components of the model resulting in a prestressed structural stability. A baseline value of 1% strain is used, with 0.1% and 5% used also to investigate the effect of prestress.

Quantitative confirmation of the model is addressed by subjecting the model to loading conditions that replicate indentation by atomic force microscopy. Two approaches are adopted to simulate the indentation of an atomic force microscope probe into the surface of the model:

(i) Application of a point load on a node to investigate differences between the point load and probe modelling methods (see (ii) below). Indentation depths resulting from a point load of 1 pN (applied to node A in Fig. 10 are compared to the reaction forces that resist applied displacements on nodes (60 nm) in the same region of the mesh. Variations in compliance along the model surface are assessed by applying a larger indentation force of 50 pN to nodes at three points along the model surface (B – D in Fig. 10.

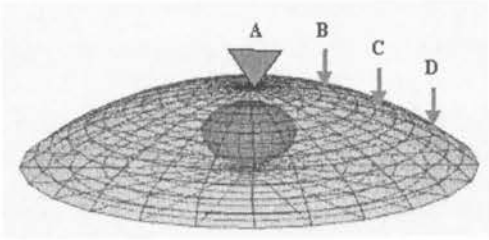

FIGURE 10. Loading conditions used for model confirmation: prescribed displacements and a point load are both applied at location A in a refined area of the surface mesh, to allow comparisons between both methods. Point loads are also applied at locations B – D along the model surface (B and D are 6 and 4 μm respectively from receptor node C).

(ii) Application of displacement boundary conditions to a number of nodes to better simulate the effect of an indenter. This allows comparisons with force-indentation curves obtained experimentally. Vertical dis-

placement boundary conditions are chosen to reflect the actual geometry of a conical probe with a contact angle of 50° as it indents the cell surface. The prescribed displacement applied in modelling the probe, ranging from 50 – 100 nm, are applied to nodes in an area of the mesh that has been refined for that purpose (in the region of node A in Fig. 10). The reaction forces resisting these indentation constraints will yield force-deflection curves that can be used in determining local elasticity values through use of an appropriate theoretical relation.

4.5. Theoretical analysis of indentation

The problem of contact between isotropic elastic bodies was first addressed by Hertz and later by Boussinesq. Sneddon (1965) followed Boussinesq's classical elasticity approach and developed expressions for the relation between load and infinitesimal indentation of a semi-infinite elastic material for several axisymmetric rigid indenter geometries. As derived by Sneddon (1965), the total load F required for normal penetration δ of a cone of semi-vertical angle α is given by:

$$F = \frac{\pi \mu r^2}{(1-\upsilon)} \tan \alpha, \tag{4.1}$$

where $\mu = \frac{E}{2(1+\upsilon)}$ is the rigidity modulus, ν is Poisson's ratio, and the contact radius r is related to indentation depth δ by:

$$r^2 = \frac{4\delta^2}{\pi^2 \tan^2 \alpha}.$$

Substituting for μ, and r gives the relation between force and indentation depth:

$$F = \frac{2E}{\pi (1-\upsilon^2) \tan \alpha} \delta^2. \tag{4.2}$$

In the approach taken in this paper, the axial component of the total reaction force at all nodes to which displacement constraints are applied is taken as equivalent to F (cell-substrate reaction forces are considered negligible in accordance with the assumption of infinite sample thickness used in the derivation of Eqs. (4.1) and (4.2): see Sneddon (1965), δ is the applied indentation, and α is taken as 50°. The expression cannot yield both the elastic modulus E and Poisson's ratio ν from the force-deflection (F vs. δ) curves; ν is therefore chosen to have a value of 0.37, identical to the underlying cytoplasm. Using Eq. (4.2), the reaction force versus applied indentation depths can then be used to determine E values.

4.6. Results – indentation

Point load indentation [(i) above] computes elasticity values lower than those obtained by modelling the actual probe geometry [(ii) above]. An applied point load of 1 pN penetrates to a depth of 51.5 nm, whereas a reaction force of $\sim$ 2 pN resists indentation constraints of 60 nm (Fig. 11).

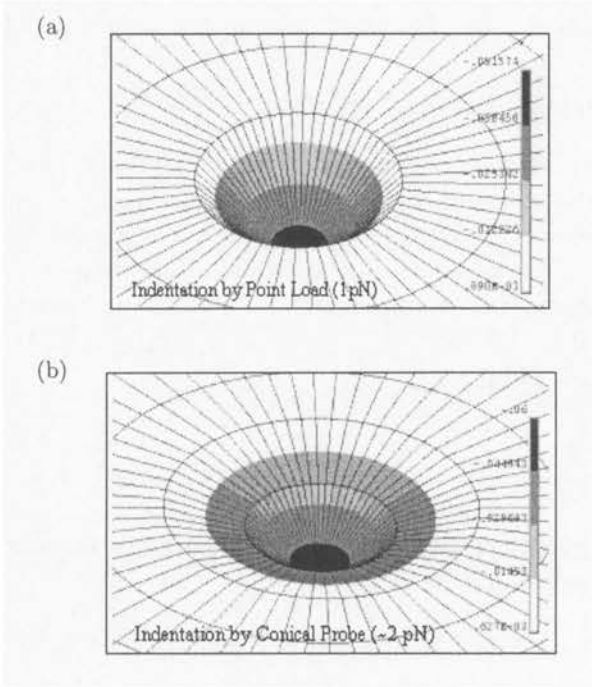

FIGURE 11. Illustration of differences in point load and probe modelling methods: (a) a point load of 1 pN causes indentation depth of 52 nm (0.0515 μm), and (b) applied indentation of 60 nm (0.06 μm) is resisted by a reaction force of 2 pN, at the same location (node A).

Proceeding with the (more realistic) probe modelling method it was found that applied indentations ranging from 50 – 100 nm are resisted by reaction forces ranging from 1 – 8 pN when a prestress value of 1% is used (see Fig. 12).

On relating these results to local elasticity estimates (Eq. 4.2) for three prestress values it is found that E values range from 0.6 to 1.4 kPa, with increases in elastic resistance as indentation depth increases (Fig. 9). Increases in the arbitrary prestress values also result in a tendency towards increases in elasticity at the point of indentation. Point load application at locations B, C, and D (see Fig. 10) yield significant differences, there is a significant increase in rigidity if indentation occurs near to or at a receptor site. For

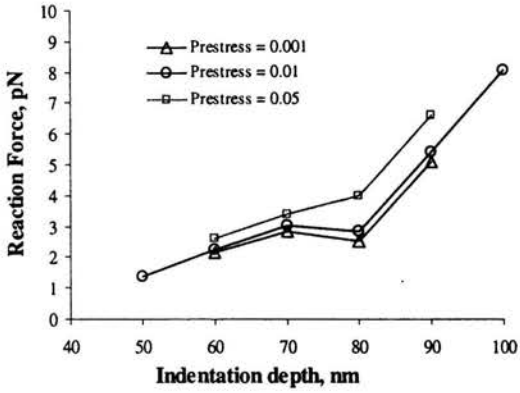

FIGURE 12. Graph of indentation depth versus reaction force along the surface of the model for three arbitrary prestress values.

example, in Fig. 9, node C is a receptor site and the indentation for 50 pN is $\sim 34\,\mu$m, node B is $\sim 6\,\mu$m from this receptor site and indentation is $116\,\mu$m with the same applied force.

4.7. Results – modelling in vitro experiments

It is also interesting to investigate how the cell is deformed and stressed during tissue culture experiments. Mullender et al. (2002) carried out experiments on monolayers of osteoblasts in both *in vitro* fluid flow and substrate strain experiments. If the osteoblasts are assumed in no way constrained by neighbouring osteoblasts, it is justifiable to model the in vitro experiments with individual models of adherent cells as described above.

4.7.1. Application of the model to substrate strain *in vitro* experiment. In the substrate strain apparatus the height of the spread osteoblasts ($\sim 5\,\mu$m) is considerably less than the thickness of the coverslip ($200\,\mu$m); when the substrate bends the tensile strain developed in the substrate to which the osteoblasts adhere is calculated to be $1{,}000\,\mu\varepsilon$ and was subsequently confirmed by strain gauge measurements (Mullender et al. 2002). The most spread model is attached to a deformable substrate by merging of neighbouring nodes on both cell and substrate. The substrate is meshed using three hexahedral brick elements through the thickness and deformed to 0.1% strain (corresponds to a half-cycle of the actuator) via displacement boundary conditions applied to nodes on opposite ends of the substrate mesh.

4.7.2. Application of the model to fluid flow *in vitro* experiment. Regarding the fluid flow experiment, since the dimensions of the adherent osteoblasts are small relative to the distance between the parallel plates, the shear stress to which the cells are subjected is assumed a constant value equal to the shear stress at the wall. This value is reported to be 0.6 Pa by Mullender et al. (2002). The modelling approach adopted assumes that the flow over the monolayer of osteoblasts is laminar and steady, and that the shear stress acts along the cell surface in the direction of flow. The total magnitude of the applied force is taken as the shear stress value at the wall divided by the area of membrane exposed to the shear stresses, giving a force of 8.47 pN applied to each node (resolved to x and y directions to ensure force is effectively tangential to cell surface), and is considered equivalent to equal distribution of a shear stress of 0.6 Pa along the model surface in the direction of flow.

When these experiments are conducted it is found that the response of the cells to the fluid flow and substrate strain stimuli differs considerably. It is easy to appreciate why this is the case if the analysis of the cells is considered because the maximum cell membrane displacement is predicted to occur in different areas of the cell, see Fig.13.

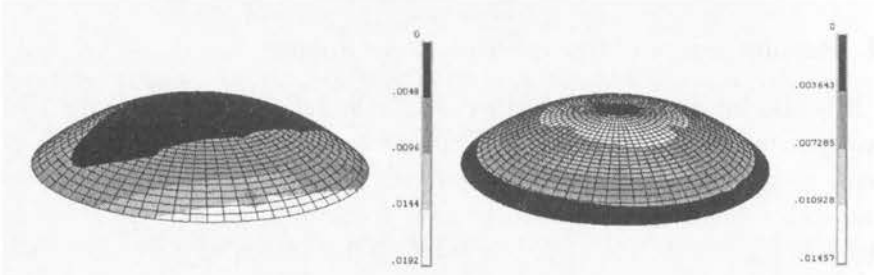

FIGURE 13. Contour plots of deformation (μm) due to substrate strain (left), and fluid flow (right).

It is also interesting to consider nuclear forces because it can be hypothesised that the expression of proteins (either signalling molecules or matrix molecules) could be influenced by this. Significantly, the stresses in the nucleus of the osteoblasts under fluid flow are found to be many times higher than those in the cells subjected to substrate strain, see Fig.14.

5. Discussion

The maintenance of life in a gravitational field relies on the fact that living organisms have evolved tissues (biological materials) that can resist

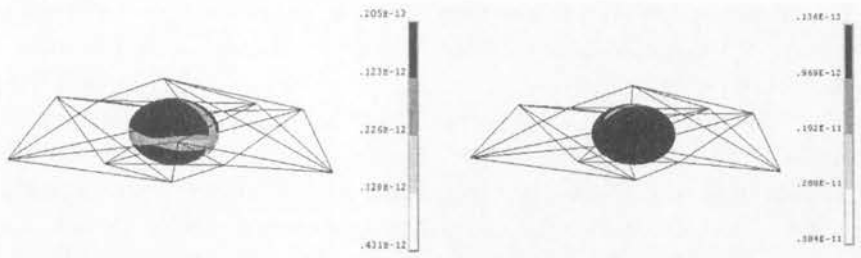

FIGURE 14. Contour plots of von Mises stress ($N/\mu m^2$) in the nucleus due to substrate strain (left), and fluid flow (right).

mechanical forces. These biological materials have, under the selection pressures of evolution, combined to form musculo-skeletal structures controlled by the central nervous system. These structures are capable gathering food, surviving, reproducing and, in the end, continuing the species. The regulation of tissue biology in response to mechanical forces plays a central role in this achievement. For this reason, questions about how tissues are mechano-regulated are of fundamental importance across a range of disciplines. This paper has attempted to illustrate how we, and others, have attempted to use computational modelling of mechanics to investigate some of the ways in which cells are involved in creating and sustaining tissues by responding to mechanical forces. Below, some issues relative to these analyses are discussed.

5.1. Analysis of tissue differentiation

Besides being of interest for fundamental reasons, computational mechanobiology can also play a role in the design of load-bearing implants, such as orthopedic and cardiovascular devices. These implants alter the stress distribution in the tissue around them, and prediction of the reaction of the tissues to the stress change is of central importance in implant design and optimization.

Clearly the above scheme for simulation of mechanoregulation of tissues contains a series of hypotheses about how cells react to physical stimuli: first Eq. (3.1) assumes that the cells disperse according to a diffusion equation which may not be true if the cells are convected into the regenerating region by blood flow or if they crawl in response to chemoattractants (Murray, 1993). Equation (3.1) also simplifies the stimulus to mitosis (cell division $\equiv$ proliferation) to a mechanical stimulus S and this is certainly a simplification. Equations (3.4) and (3.5) suggest that the same stimulus mechano-regulates mitosis as for and stem cell differentiation.

Of the issues that warrant further research, one of the most interesting is the nature of the biophysical stimulus. Carter & Beaupré (2001) propose hydrostatic and deviatoric stresses in an elastic model of the tissue and Kuiper et al. (2000) derive fluid shear stresses as a stimulus. Either of these may be superior to the one presented here. Furthermore, tensorial representations of the stimulus (e.g. Doblaré et al., 2002) give a better representation of the complexity of tissue adaptation. Micromechanical finite element models which allow the computation of the stimulus as a function of the local microstructure are needed if the results on cell experiments are to be used to predict changes in apparent level properties. In fact, this is one of the most pressing problems to be solved in computational mechanobiology, in our opinion.

The relationship between mechanical stimulus in a tissue and the rate of formation or resorption presented in Fig. 3 is quite speculative. The only part that has been explored with rigor to date is $S < S_c$, *i.e.*, the part dealing with the resorption, homeostasis, and deposition of bone. However, if these methods are to find use in the new discipline of tissue engineering, the other parts of this relationship will need to be developed. This will require close collaboration between cell and molecular biologists, applied mechanicians, and tissue histologists in a broad interdisciplinary collaboration.

5.2. Analysis of adherent cells

In our analysis of single cell stimulation, we attempt to account for the structurally relevant components of a cell, while incorporating non-linear aspects of adherent cell behaviour that are due to the interconnected actin and microtubules in the cytoskeleton.

The material properties chosen to represent the cytoskeleton have been used in previous models (Stamenovic and Coughlin, 2000), while similar values for flexural rigidity have been estimated theoretically (Ben-Avraham and Tirion, 1995), and are in agreement with other experimental work (Tsuda et al., 1996). Also, Shin and Athanasiou (1999) have reported a value of 0.37 for Poisson's ratio of an anchored osteoblast using a linear biphasic finite element analysis to curve-fit experimental data obtained by a cytoindentation method, while other experimental studies (Mathur et al., 2001) and theoretical models (Kamm et al., 2000) use values of up to > 0.49 to describe cytoplasm incompressibility (it is considered composed of 70% water). Future parameter studies will suggest the influence of this value on cell structural behaviour.

A benefit of the modelling approach used in this paper is that the rearrangement performed on the tensegrity-based cytoskeleton reflects struc-

tural changes that occur within the cell during spreading. In living cells, the orientation, positioning and length of internal cytoskeletal components is altered by polymerisation, and by clustering of actin filaments. During spreading adhesion bonds are formed between internal structural proteins (e.g. vinculin and talin) and extra-cellular proteins (e.g. fibronectin) that influence positioning of the internal components. It has been suggested by Gittes et al. (1993) that to account for the seemingly excessively rigid mechanical properties measured, sliding and movement may occur between filaments and tubules. An additional justification for attributing a dominant role to the cytoskeleton is based on the hypothesis that many enzymes and molecules, which physically associate with the insoluble components of the cytoskeleton and the extracellular matrix, mediate cell function such as DNA or RNA synthesis, and signal transduction.

Regarding model confirmation, it was necessary to mesh the model with hexahedral elements that use linear shape functions since it was found that displacement boundary conditions applied to nodes of tetrahedral elements resulted in significant warping of those elements. Sweep meshing with hexahedral elements resulted in a nodal density on the top surface that was sufficiently refined for application of constraints that reflect the probe geometry at each indentation depth. Further refinement would lead to a greater number of nodes and hence increased accuracy, but was avoided due to technical difficulty and computational expense.

The validity of applying the expressions derived by Sneddon has been discussed by other authors (Costa and Yin, 1999). The expressions are based on the assumption of infinite sample thickness. Since the indentation depths ($< 100\,\text{nm}$) are significantly less than the height of the cell model ($\sim$7000 nm), this condition is considered adequately satisfied. The load-indentation relation used here (Eq. 4.2) is in agreement with that used by both Weisenhorn et al. (1993) and Charras and Horton (2002). It has, however, been suggested by Costa and Yin (1999) that the assumption that strains are infinitesimal is not valid when applied via a conical or pyramidal tip with a contact angle of $< 45°$, suggesting that finite strains most likely occur in the contact region. Hence a large displacement contact analysis would perhaps more accurately reflect material behaviour on probe indentation. Considering Eq. (3.2), the probe contact angle chosen for the analysis presented in this paper will have a significant bearing on elasticity results, but is in the range of angles ($35° - 50°$) used in those experimental measurements to which comparisons are made in Sec. 5.2.1 below. The indentation depths applied via displacement constraints are also in the range of those applied experimentally, i.e. (from $10 - 100\,\text{nm}$ in Mathur et al., 2001), but the upper limit is restricted as the hexahedral elements begin to warp for $\delta > 110\,\text{nm}$. Other

limitations of the approach are related to the fact that elasticity under an indenting probe may be constantly changing, and that material behaviour is viscoelastic (Sato et al., 1990).

5.2.1. Comparisons with experimental AFM results. The point load modelling method yields lower values of elasticity than probe modelling (Fig. 11). It is therefore shown that the point method is not satisfactory since the angle of contact is infinitesimally small when a point load is applied on a single node, and does not accurately reflect the geometry of the probe that transmits the indenting force.

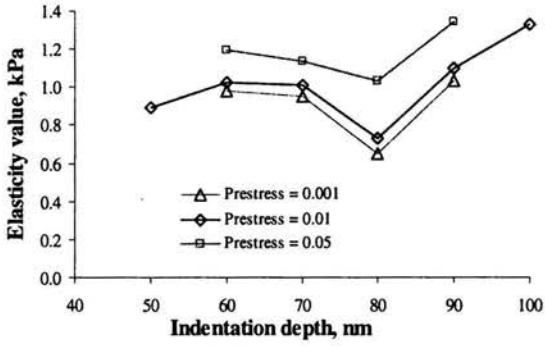

FIGURE 15. Graphs of indentation depth versus local elasticity values along the surface of the model for three arbitrary prestress values.

Regarding the probe modelling method, the elasticity values obtained (Fig.15; 0.6–1.4 kPa) from the indentation versus reaction force data (Fig. 12) are in the range of those determined experimentally for fibroblasts using micromanipulation (0.6 – 1 kPa) (Kelly and Prendergast, 2003), using micropipette aspiration of chondrocytes (0.6 kPa) (Klein-Nulend et al., 1996), and lower than those reported using AFM (2.1–8.8 kPa) on osteoblasts (Kaspar et al., 2000).

Charras and Horton (2002) reported similar average values for osteoblasts also using AFM, while recording peak local elasticity values of up to 100 kPa due to presence of stress fibres. Other papers (Radmacher et al., 1996; Thoumine et al., 1999; Domke et al., 2000) have also reported such large differences in elasticity when probing at various locations along the cell surface. Similarly, in our model we find that compliance varies considerably along the surface (Fig.16). Indentation at more rigid receptor sites in our model would result in elasticity values closer to the peak values reported in Charras and Horton (2002). Increases in the prestress value applied to the microfilament

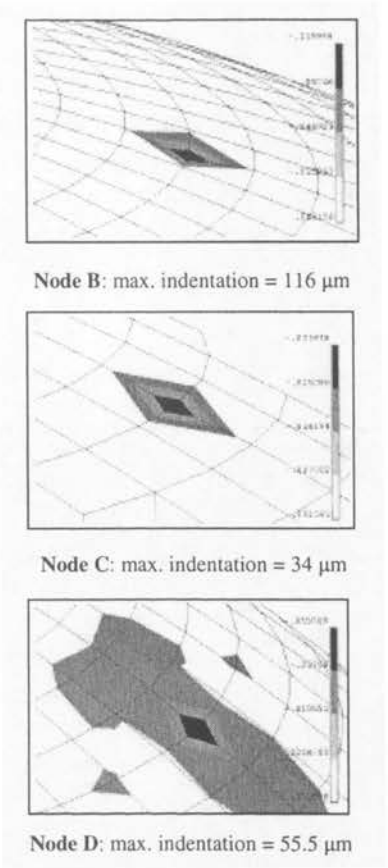

FIGURE 16. Contour plots of displacements caused by application of a point load of 50 pN at nodes (B – D) along the model surface as illustrated in Fig. 6. Prestress value is 0.01 (1%).

elements in our model also result in significant increases in elasticity values (Fig.15; it should be noted that, at an indentation location nearer to a receptor site, these prestress effects would be increasingly noticeable due to the underlying cytoskeleton). However, the increases in rigidity due to position of indentation along the model surface have a larger bearing on elasticity than does the prestress value within the microfilaments.

5.2.2. Future uses of the model. By altering parameters, the model may be used to explore the origin of observed non-linear aspects of adherent cell behaviour, such as increases in stiffness in spreading fibroblasts, contentious issues such as the proportion of compression borne by microtubules in adherent cells, and the importance of cytoplasm incompressibility.

The response of adherent cells to mechanical stimuli of various kinds (substrate strain, fluid flow) in culture has been the subject of many studies, e.g. Bakker et al. (2001) and Owan and Burr (1997). It has never been possible to fully characterise the effect of various stimuli on cell deformation. Given that the present model has been confirmed against AFM experiments, loading conditions that reflect the mechanical strains imposed on adherent cells *in vitro* may be applied to it, allowing computation of cell deformation and possible suggestions as to the biomechanical origins of differences in observed cell behaviour.

Comparison of results from different *in vitro* experiments have, in the past, been difficult, preventing speculation as to the possible mechanisms by which applied mechanical strains are converted to biochemical signals that alter cell function. The computational models presented here show larger displacement of the cytoskeleton in fluid flow compared to substrate strain; this may be of significance because it has been hypothesised that the cytoskeleton may form a physical pathway for transmitting deformation and transduction of signals from adhesion sites to the nucleus where gene expression is regulated (Maniotis & Chen, 1999). The resultant straining of cytoskeleton-substrate attachments such as adhesion sites may be involved in the production of NO and PGE_2 signalling molecules through stimulation of intra-extra-cellular proteins, or receptor-ligand molecules. Furthermore, in the fluid flow model, the principal stress in the nucleus many times higher than due to substrate strain. This higher stressing of the nucleus may also be significant because transcription factors that regulate gene expression may be produced on stimulation of the nucleus.

6. Conclusion

Modelling the processes carried out by cells – such as tissue growth, remodelling and adaptation – has most often been done without explicit modelling of cell activity using classical continuum mechanics. However it may be noted that such approaches require many empirical constants reducing the testability of hypotheses derived from them (Prendergast, 2001). More recent studies have used numerical approaches to aggregate the mechanoregulated response of cells, where a volume of the tissue is represented as an element a finite element model, see Sec. 2 above. These methods have the advantage of bringing biological control mechanisms into the model but have the disadvantage (in some peoples eyes) of not being a solution to a pointwise equation. The extrapolation of these "cell-based" approaches to the level of the individual cell can be envisaged if the cell itself is modelled using the kind of approach presented in Sec. 4 of this paper. Although it would be compu-

tationally expensive, explicit modelling of the migration and differentiation of cell populations in response to mechanical stimuli would open a new vista in biomechanical research.

Acknowledgements

Financial support for this research is partly provided by the Program for Research in Third Level Institutions (PRTLI) of the Higher Education Authority in Ireland. The authors gratefully acknowledge the EU funded BITES (Biomechanical Interactions in Tissue Engineering and Surgical Repair) project, under part of what is reported above has been funded (Contract no. QLK3-1999-00559).

References

1. A-HASSAN, E., W.F. HEINZ, M.D. ANTONIK, N.P. D'COSTA, AND S. NAGESWARAN, Relative microelastic mapping by AFM, *Biophysical Journal*, Vol.74, pp.1564-1578, 1998.
2. ASCNEZI, A., Biomechanics and Galilei Galileo. *Journal of Biomechanics*, Vol.26, pp.95-99, 1993.
3. A.D. BAKKER, K. SOEJIMA, J. KLEIN-NULEND, E. BURGER, The production of nitric oxide and prostaglandin E_2 by primary bone cells is shear stress dependent, *Journal of Biomechanics*, Vol.34, pp.671-677, 2001.
4. D. BEN-AVRAHAM, M.M. TIRION, Dynamic and Elastic Properties of F-actin: a normal modes analysis, *Biophysical Journal*, Vol.68, pp.1231-1245, 1995.
5. P. BIANCO, P.G. ROBEY, Stem cells in tissue engineering, *Nature* Vol.414, 118-212, 2001.
6. G. BINNIG, C.F. QUATE, C. GERBER, Atomic force microscope, *Physical Review Letters*, Vol.56, 9, pp.930-933, 1986.
7. N. CAILLE, O. THOUMINE, Y. TARDY, J. J. MEISTER, Contribution of the Nucleus to the mechanical properties of endothelial cells, *Journal of Biomechanics*, Vol.35, pp.177-187, 2002.
8. A.I. CAPLAN, The mesengenic process, *Clinics in Plastic Surgery*, Vol.21, pp.429-435, 1994.
9. D.R. CARTER, Mechanical loading histories and cortical bone remodelling, *Calcified Tissue International* Vol.36, pp.19-24, 1984.
10. D.R. CARTER, G.S. BEAUPRÉ, Skeletal Function and Form. Mechanobiology of Skeletal Development, Aging, and Regeneration, *Cambridge University Press: Cambridge*, 2001.
11. G. T. CHARRAS, M.A. HORTON, Determination of cellular strains by combined atomic force microscopy and finite element modelling. *Biophysical Journal*, Vol.83, pp.858-879, 2002.

12. K.D. COSTA, F.C. YIN, Analysis of indentation: implications for measuring mechanical properties with the atomic force microscope, *ASME Journal of Biomechanical Engineering*, Vol.121, pp.462-471, 1999.

13. S.C. COWIN, Bone poroelasticity, *Journal of Biomechanics*, Vol.32, pp.217-238, 1999.

14. S.C. COWIN, D.H. HEGEDUS, Bone remodelling I: theory of adaptive elasticity, *Journal of Elasticity*, Vol.6, pp.313-326, 1976.

15. M. DOBLARÉ, J.M. GARCIÁ, J. CEGOÑINO, Development of an internal bone remodelling theory and applications to some problems in orthopaedic biomechanics, *Meccanica*, Vol.37, pp.365-374, 2002.

16. J. DOMKE, S. DANNOHL, W.J. PARAK, O. MÜLLER, W.K. AICHER, AND M. RADMACHER, Substrate dependent differences in morphology and elasticity of living osteoblasts investigated by atomic force microscopy, *Colloids and Surfaces B: Biointerfaces*, Vol.19, pp.367-379, 2000.

17. E. EVANS, A. YEUNG, Apparent viscosity and cortical tension of blood granulocytes determined by micropipette aspiration, *Biophysical Journal*, Vol.56, pp.151-160, 1989.

18. T. FRISCH, O. THOUMINE, Predicting the kinetics of cell spreading, *Journal of Biomechanics*, Vol.35, pp.1137 - 1141, 2002.

19. Y.C. FUNG, *Foundations of Solid Mechanics*, Prentice-Hall, Englewood Cliffs, p. 360, 1965.

20. F. GITTES, B. MICKEY, J. NETTLETON, J. HOWARD, Flexural rigidity of microtubules and actin filaments measured from thermal fluctuations in shape, *Journal of Cell Biology*,Vol.120, 4, pp.923-934, 1993.

21. F. GITTES, B. MICKEY, Flexural rigidity of microtubules and actin filaments measured from thermal fluctuations in shape. *Journal of Cell Biology* Vol.120, 4, pp.923-934, 1993.

22. F. GUILAK, V.C. MOW, The mechanical environment of the chondrocyte: a biphasic finite element model of cell-matrix interactions in articular cartilage, *Journal of Biomechanics,* Vol.33, 12, pp.1663-1673, 2000.

23. F. GUILAK, J.R. TEDROW, R. BURGKART, Viscoelastic properties of the cell nucleus, *Biochemical and Biophysical Research Communications*, Vol.269, 3, pp.781- 786, 2000.

24. F. GUILAK, C. MOW, The mechanical environment of the chondrocyte: a biphasic finite element model of cell-matrix interactions in articular cartilage, *Journal of Biomechanics* Vol.33, 12, pp.1663-1673, 2000.

25. E. HENDERSON, P.G. HAYDON, D.S. SAKAGUCHI, Actin filament dynamics in living glial cells imaged by atomic force microscopy, *Science*, Vol.257, pp.1944-1946, 1992.

26. R.M. HOCHMUTH, Micropipette aspiration of living cells, *Journal of Biomechanics*, Vol.33, 1, pp.15-22, 2000.

27. R. HUISKES, R. RUIMERMAN, G.H. VAN LENTHE, J.D. JANSSEN, Effects of mechanical forces on maintenance and adaptation of form in trabecular bone, *Nature*, Vol.405, pp.704-706.

28. R. HUISKES, W.D. VAN DRIEL, P.J. PRENDERGAST, K. SØBALLE, A biomechanical regulatory modelfor peri-prosthetic tissue formation, *Journal of Materials Science: Materials in Medicine,* Vol.8, 785-788, 1997.

29. D.E. INGBER, Cellular tensegrity: defining new rules of biological design that govern the cytoskeleton, *Journal of Cell Science*, Vol.104, pp.613-627, 1995.

30. C.R. JACOBS, M.E. LEVENSTON, G.S. BEAUPRÉ, J.C. SIMO, D.R. CARTER, Numerical instabilities in bone remodelling simulations: the advantages of a node-based finite element approach, *Journal of Biomechanics*. Vol.28, 449-459, 1995.

31. R. D. KAMM, A.K. MCVITTIE, M. BATHE, On the role of continuum models in mechanobiology. *ASME 2000 Mechanics in Biology*, Vol.242, pp.1-11, 2000.

32. R.D. KAMM, A.K. MCVITTIE, M. BATHE, On the role of continuum models in mechanobiology, *ASME Mechanics in Biology*, Vol.242, pp.1-11, 2000.

33. D. KASPAR, W. SEIDL, C. NEIDLINGER-WILKE, A. IGNATIUS, L. CLAES, Dynamic cell stretching increases human osteoblast proliferation and CICP synthesis but decreases osteocalcin synthesis and alkaline phosphatase activity, *Journal of Biomechanics*, Vol.33, pp.45-51, 2000.

34. D.J. KELLY, P.J. PRENDERGAST, The poor quality of repair tissue that forms in osteochondral defects can be attributed to the local mechanical environment within the defect, In *Proceedings of the 9th Bioengineering in Ireland Conference*, (Eds., D.P. FitzPatrick et al.), p. 75, 2003.

35. J. KLEIN-NULEND, C.M. SEMEINS, E.H. BURGER, A. VAN DER PLAS, N.E. AJUBI , P.J. NIJWEIDE, Response of isolated osteocytes to mechanical loading in vitro, In: A. Odgaard, H. Weinans, Eds., *Bone Structure and Remodelling*, World Scientific, Singapore, pp.37-49, 1996.

36. J.H. KUIPER, B.A. ASHTON, J.B. RICHARDSON, Computer simulation of fracture callus formation and stiffness restoration. In: *Proceedings of the European Society of Biomechanics*, Royal Academy of Medicine in Ireland: Dublin, (Eds., P.J. Prendergast, T.C. Lee, A.J. Carr), p 61. (www.biomechanics.ie/esb2000), 2000.

37. D. LACROIX, P.J. PRENDERGAST, A mechano-regulation model for tissue differentiation during fracture healing: analysis of gap size and loading, *Journal of Biomechanics* Vol.35, 1163-1171, 2002a.

38. D. LACROIX, P.J. PRENDERGAST, Three-dimensional simulation of fracture repair in the human tibia, *Computer Methods in Biomechanics and Biomedical Engineering* Vol.5, 369-376, 2002b.

39. D. LACROIX, P.J. PRENDERGAST, G. LI, D. MARSH, Biomechanical model to simulate tissue differentiation and bone regeneration: application to fracture healing, *Medical and Biological Engineering and Computing* Vol.40, pp.14-21, 2002.

40. A. MANTIOTIS, C. CHEN, demonstration of mechanical connections between integrins, cytoskeletal filaments, and nucleoplasm that stabalise nuclear structure. *Proc. Natl. Acadamy of Science (USA)*, Vol.94, 849-854, 1997.

41. A.B. MATHUR, A.M. COLLINSWORTH, W.M. REICHERT, W.E. KRAUS, G.A. TRUSKEY, Endothelial, cardiac muscle and skeletal muscle exhibit different viscous and elastic properties as determined by atomic force microscopy, *Journal of Biomechanics*, Vol.34, pp.1545-1553, 2001.

42. V.C. MOW, S.C. KUEI, W.M. LAI, C.G. ARMSTRONG, Biphasic creep and stress relaxation of articular cartilage: theory and experiments. *Journal of Biomechanical Engineering* Vol.102, pp.73-84, 1980.

43. M. MULLENDER, A. J. EL HAJ, Y. YANG, J. MAGNAY, M. A. VANDUIN, J. KLEIN-NULEND, Cyclic strain and fluid flow induce different responses in human bone cells. *Proc. IV World Congress of Biomechanics*, Calgary, Canada, 2002.

44. J.D. MURRAY, *Mathematical Biology*, Springer, 2nd Edn., pp.232-236, 1993.

45. I. OWAN, D.B. BURR, C.H. TURNER, J. QUI, Y. TU, J.E. ONYIA, R.L. DUNCAN, Mechanotransduction in bone: osteoblasts are more sensitive to fluid forces than mechanical strain, *American Journal of Applied Physiology* Vol.273 (Cell Physiology Vol.42), pp.C810-815, 1997.

46. I. OWAN, D. BURR, Mechanotransduction in bone: osteoblasts are more responsive to fluid forces than mechanical strain, *American Journal of Physiology, Cell Physiology*, Vol.273, 42, pp.810 - 815, 1997.

47. P.J. PRENDERGAST, An analysis of theories in biomechanics. *Engineering Transactions* Vol.49, 117-133, 2001.

48. P.J. PRENDERGAST, Mechanics applied to skeletal ontogeny and phylogeny, *Meccanica* Vol.37, pp.317-334, 2002.

49. P.J. PRENDERGAST, R. CONTRO, *Meccanica* Vol.37, (Special Issue) 4/5, 2002.

50. P.J. PRENDERGAST, R. HUISKES, K. SØBALLE, Biophysical stimuli on cells during tissue differentiation at implant interfaces. *Journal of Biomechanics* Vol.30, pp.539-548, 1997.

51. P.J. PRENDERGAST, D. TAYLOR, Prediction of bone adaptation using damage accumulation, *Journal of Biomechanics*, Vol.29, pp.1067-1076, 1994.

52. P.J. PRENDERGAST, M.C.H. VAN DER MEULEN, Mechanics of bone regeneration, In: S.C. Cowin, Ed., *Bone Mechanics Handbook*, pp.25-1 to 25-18, CRC Press, Boca Raton, 2001.

53. M. RADMACHER, M. FRITZ, C. RACHER, J.P. CLEVELAND, P.K. HANSMA, Measuring the viscoelastic properties of human platelets with the atomic force microscope, *Biophysical Journal*, Vol.70, pp.556-567, 1996.

54. M. SATO, D.P. THERET, L.T. WHEELERM, N. OHSHIMA, R.M. NEREM, Application of the micropipette technique to the measurement of cultured porcine aortic endothelial cell viscoelastic properties, *ASME Journal of Biomechanical Engineering*, Vol.112, pp.263-268, 1990.

55. D. SHIN, AND K. ATHANASIOU, Cytoindentation for obtaining cell biomechanical properties, *Journal of Orthopaedic Research*, Vol.17, 6, pp.880-890, 1999.

56. I.N. SNEDDON, The relation between load and penetration in the axisymmetric Boussinesq problem for a punch of arbitrary profile, *International Journal of Engineering Science*, Vol.3, pp.47-57, 1965.

57. D. STAMENOVIC, M.F. COUGHLIN, A quantitative model of cellular elasticity based on tensegrity, *Journal of Biomechanical Engineering*, Vol.122, pp.39-43, 2000.

58. D. STAMENOVIC, M.F. COUGHLIN, The role of prestress and architecture of the cytoskeleton and deformability of cytoskeletal filaments in mechanics of adherent cells: a quantitative analysis, *Journal of Theoretical Biology*, Vol.201, pp.63-74, 1999.

59. O. THOUMINE, A. OTT, Time scale viscoelastic and contractile regimes in fibroblasts probed by microplate manipulation, *Journal of Cell Science*, Vol.110, pp. 2109-2116, 1997.

60. O. THOUMINE, O. CARDOSO, Changes in the mechanical properties of fibroblasts during spreading: a micromanipulation study, *European Biophysical Journal*, Vol.28, 3, pp.222-234, 1999.

61. O. THOUMINE, O. CARDOSO, J.J. MEISTER, Changes in the mechanical properties of fibroblasts during spreading: a micromanipulation study, *European Biophysical Journal, EBJ*, Vol.28, 3, pp.222-234, 1999.

62. Y. TSUDA, H. YASUTAKE, A. ISHIJIMA, T. YANAGIDA, Torsional rigidity of single actin filaments and actin bond breaking force under torsion measured directly by *in vitro* micromanipulation, *Proc. of the National Academy of Sciences of the USA*, Vol.93, pp.12937-12942, 1996.

63. M.C.H. VAN DER MEULEN, R. HUISKES, Why mechanobiology? A survey article, *Journal of Biomechanics* Vol.35, 401-414, 2002.

64. N. WANG, K. NARUSE, D. STAMENOVIC, Mechanical behaviour in living cells consistent with the tensegrity model, *Proc. of the National Academy of Sciences of the USA*, Vol.98, No.14, pp.7765-7770, 2001.

65. H. WEINANS, R. HUISKES, H.J. GROOTENBOER, The behaviour of adaptive bone remodelling simulation models, *Journal of Biomechanics*, Vol.25, pp.1425-1441, 1994.

66. H. WEINANS, P.J. PRENDERGAST, Tissue adaptation as a dynamical process far from equilibrium, *Bone*, Vol.19, pp.143-149, 1996.

67. A.L. WEISENHORN, M. KHORSANDI, S. KASIAS, V. GOTZOS, H. BUTT, Deformation and height anomaly of soft surfaces studied with an AFM, *Nanotechnology*, Vol.4, pp.106-113, 1993.

68. S. WENDLING, C. ODDOU, D. ISABEY, Stiffening Response of a Cellular Tensegrity Model, *Journal of Theoretical Biology*, Vol.196, pp.309-325, 1999.